ENTROPY PRODUCTION AT ALL SCALES

M. Valorani* and S. Paolucci**
mauro.valorani@uniroma1.it
*Mechanical and Aerospace Engineering, Sapienza University of Rome, Italy
**Aerospace and Mechanical Engineering, University of Notre Dame, IN, USA

Abstract
Spatially homogeneous systems are characterized by the simultaneous presence of a wide range of time scales. When the dynamics of such reactive systems develop very-slow and very-fast time scales separated by a range of active time scales, with large gaps in the fast/active and slow/active time scales, then it is possible to achieve multi-scale adaptive model reduction along-with the integration of the governing ordinary differential equations using the G-Scheme framework. The G-Scheme assumes that the dynamics is decomposed into active, slow, fast, and when applicable, invariant subspaces. We derive the expressions that express the direct link between time scales and entropy production by resorting to the estimates provided by the G-Scheme. With reference to a constant volume, adiabatic batch reactor, we compute the contribution to entropy production by the four subspaces. The numerical experiments show that, as indicated by the theoretical derivation, the contribution to entropy production of the fast subspace is of the same magnitude of the error threshold chosen for the numerical integration, and that the contribution of the slow subspace is generally much smaller than that of the active subspace.

Introduction

The numerical solution of mathematical models for reaction systems in general, and reacting flows in particular, is a challenging task because of the simultaneous contribution of a wide range of time scales to the systems' dynamics. However, it is typical that the dynamics can develop very-slow and very-fast time scales separated by a range of active time scales.

An opportunity to reduce the complexity of the problem arises when the gaps in the fast/active and slow/active time scales become large. In [1], we provided an asymptotic analysis and proposed a numerical technique consisting of an algorithmic framework, named the G-Scheme, to achieve multi-scale adaptive model reduction along-with the integration of ordinary differential equations (ODEs) using objective criteria. In the G-Scheme, it is assumed that the dynamics is (locally) decomposed into active, slow, fast, and when applicable, invariant subspaces. The method is directly applicable to initial-value ODEs and (by using the method of lines) to partial differential equations (PDEs).

For irreversible (non-equilibrium) multi-scale processes, such as a detailed kinetic model (DKM), one question not addressed in [1] is how does the entropy production relate to the decomposition into fast, active, slow, and invariant subspaces. A quick qualitative answer could be obtained by establishing a correspondence among fast, active, slow, and invariant subspaces with near-equilibrium, non-equilibrium, near-frozen, and isentropic processes. Indeed, near-equilibrium and near-frozen processes are expected to be nearly isentropic (and quasi-linear), the algebraic invariants (linear and nonlinear) correspond to isentropic processes, and non-equilibrium processes are expected to be non-isentropic (and nonlinear). As a consequence, the entropic contributions of the fast and slow subspaces are expected to be small with respect to that of the active subspace. In this paper, we will analyze this aspect of the G-Scheme with the help of illustrative examples in the context of auto-ignition in a spatially homogeneous batch reactor.

Theory

We would like to verify empirically the contributions of the slow, active, and fast subspaces to the overall rate of entropy production in a system featuring chemical non-equilibrium. To this end, we resort to the standard model of a constant volume, adiabatic, batch reactor, where the mixture's temperature is initially set above the auto-ignition temperature.

The set of ODEs describing the time evolution of the state in a batch reactor at constant volume is

$$\begin{aligned} \frac{dY_j}{\mathrm{dt}} &= \frac{W_j\,\dot{\omega}_j\,(T,Y_j)}{\rho}, \quad j=1,\ldots,N, \\ \frac{\mathrm{dT}}{\mathrm{dt}} &= -\frac{1}{\rho C_p}\sum_{j=1}^{N} h_j(T) W_j \dot{\omega}_j\,(T,Y_j) \end{aligned} \tag{1}$$

where T and Y_j are the temperature and composition (expressed in term of mass fractions) of the mixture, t is time, ρ is the mixture density which is constant for the assumption of constant volume, C_p is the mixture mean heat capacity at constant pressure per unit mass, N is the number of species, h_j is the species enthalpy per unit mass, W_j is the species molecular weight, and $\dot{\omega}_j$ is the molar rate of formation/destruction of the j-th species. The set of ODEs is closed by the thermal equation of state for a mixture of ideal gases $p=\rho\,R\,T$, where p is the pressure in the reactor vessel, $R=\sum_N R_j Y_j$ is the mixture's gas constant, and the caloric equation of state can be expressed as

$$C_p\,(T,Y_j) = \sum_{j=1}^{N} C_{p,j}(T) Y_j, \tag{2}$$

where $C_{p,j}(T)$ is the heat capacity at constant pressure per unit mass of the j-th species.

The customary relations between mass fractions Y_j, molar fractions X_j, and molar concentrations c_j read:

$$c_j = \rho\,\frac{X_j}{\bar{W}} = \rho\,\frac{Y_j}{W_j}, \tag{3}$$

where $\bar{W}=\sum_N W_j X_j$ is the mean molecular weight of the mixture. The molar rate of formation/destruction of the j-th species reads:

$$\dot{\omega}_j\,(T,Y_j) = \sum_{k=1}^{K} \Delta\nu_{j,k}\,r^k\,(T,Y_j)\,, \tag{4}$$

where $\boldsymbol{\nu}'_k=\nu'_{j,k}$ and $\boldsymbol{\nu}''_k=\nu''_{j,k}$ are the forward and reverse stoichiometric coefficients of the j-th species in the k-th reaction out of K total reactions, and $\Delta\boldsymbol{\nu}_k=\Delta\nu_{j,k}=\boldsymbol{\nu}''_k-\boldsymbol{\nu}'_k$ is the net stoichiometric coefficient. The net rate of the k-th reaction reads:

$$r^k\,(T,\rho,Y_j) = \; r_f^k - r_b^k = K_f^k \prod_{j=1}^{N} c_j^{\boldsymbol{\nu}'_k} - K_b^k \prod_{j=1}^{N} c_j^{\boldsymbol{\nu}''_k} = K_f^k \prod_{j=1}^{N} \left(\rho\frac{Y_j}{W_j}\right)^{\boldsymbol{\nu}'_k} - K_b^k \prod_{j=1}^{N} \left(\rho\frac{Y_j}{W_j}\right)^{\boldsymbol{\nu}''_k} \tag{5}$$

where r_f^k and r_b^k are the forward and backward reaction rates, and K_f^k and K_b^k are the forward and backward reaction constants, which depend exponentially on temperature according to the standard Arrhenius form.

The entropy per unit mass s of a mixture of N ideal gases is given by

$$\begin{aligned} s\left(T,p,Y_j\right) &= \frac{S\left(T,p,X_j\right)}{\bar{W}} \\ S\left(T,p,X_j\right) &= \sum_{j=1}^{N}\left(S_j^0(T) - \mathcal{R}\log\left(\frac{p}{p_{\text{ref}}}\right) - \mathcal{R}\,\log\,X_j\right)X_j, \\ S_j^0(T) &= \Delta S_{f,j}^0 + \int_{T_{ref}}^{T}\frac{\bar{C}_{p,j}(T)}{T}dT \end{aligned} \tag{6}$$

with S the entropy per molar units, $\Delta S_{f,j}^0$ the species formation entropy per molar units, $\bar{C}_{p,j}$ the species molar heat capacity, and $\mathcal{R}$ the universal gas constant.

If we define the state of the system as the algebraic vector $\boldsymbol{x} = \{Y_j, T\}$ with the corresponding vector field defined as

$$\boldsymbol{g}\left(Y_j,T\right) = \left\{\frac{W_j\,\dot{\omega}_j\left(T,Y_j\right)}{\rho}, -\frac{1}{\rho C_p}\sum_{j=1}^{N}h_j\,W_j\,\dot{\omega}_j\left(T,Y_j\right)\right\}. \tag{7}$$

we can recast Eq. (1) as a dynamical system defined by the Cauchy problem

$$\begin{aligned} &\frac{\mathrm{d}\boldsymbol{x}}{\mathrm{dt}} = \boldsymbol{g}(\boldsymbol{x}), \qquad \boldsymbol{x}(0) = \boldsymbol{x}_0, \qquad \text{with} \\ &\boldsymbol{x} \in \mathbb{R}^{N+1},\ \mathrm{t} \in (0,T) \subset \mathbb{R},\ \text{and}\ \boldsymbol{g} : E \subset \mathbb{R}^{N+1} \to \mathbb{R}^{N+1}. \end{aligned} \tag{8}$$

The associated phase flow φ_t is such that $\varphi_t(\boldsymbol{x}_0)$ is the solution of the Cauchy problem at time t starting at $\boldsymbol{x}(t=0) = \boldsymbol{x}_0$.

Basic Concepts of the G-Scheme

In the G-Scheme, we assume that the dynamics can be decomposed at any given time instant into active, slow, fast, and when applicable, invariant subspaces. The G-Scheme introduces a local curvilinear frame of reference, defined by a set of orthonormal basis vectors with corresponding coordinates, attached to this decomposition. The evolution of the curvilinear coordinates associated with the active subspace, $\Delta\xi^a$, is described by non-stiff ODEs, whereas those associated with the slow, $\Delta\xi^h$, and fast, $\Delta\xi^t$, subspaces are accounted for by applying asymptotic approximations of the original problem to provide $\Delta\xi^h_{FF}$, and $\Delta\xi^t_{SIM}$, respectively.

The G-Scheme involves two main stages:

1. evolution of the active modes described by $N_{\mathbb{A}}$ non-stiff ODEs;
2. corrections associated with the slow/fast dynamics.

The active ODEs evolve in subspace $\mathbb{A}$ which is freed from fast scales, i.e., they are non-stiff. They can be solved by resorting to any explicit integration scheme (e.g., explicit Runge-Kutta). When compared to a standard BDF implicit scheme for stiff problems, the G-Scheme requires the solution of $N_{\mathbb{A}}$ explicit non-stiff ODEs instead of $N+1$ implicit stiff ODEs. However, the scheme requires the identification of the tangent space decomposition.

Ideal decomposition of the tangent space $\mathcal{T}_{\boldsymbol{x}}$ at any point $\boldsymbol{x} \in \mathbb{C} \subset \mathbb{R}^{N+1}$ involves the identification of $N+1$ invariant subspaces, a difficult task. The G-Scheme decomposes the

tangent space in four subspaces having time scales of comparable magnitude, $\mathcal{T}_x = \mathbb{E} \oplus \mathbb{H} \oplus \mathbb{A} \oplus \mathbb{T}$, where $\mathbb{E}$ is the linear subspace spanned by directions associated with invariants, if any exists (conservation laws). All scales slower than the active ones are confined to the slow subspace $\mathbb{H}$(ead) (dormant/near-frozen processes). The active subspace $\mathbb{A}$ contains all the current intermediate dynamic time scales (active/non-equilibrium). All scales faster than the active ones are confined in the fast subspace $\mathbb{T}$(ail) (exhausted/near-equilibrium). Thus, the basic concept in the G-Scheme is to 'distill' the Heart, and 'cut' the Head and Tail in a generic multi-scale dynamical system.[1]

The most important decision to be taken in the implementation of the G-Scheme framework is the choice of a curvilinear frame of reference, i.e., a basis matrix yielding a maximal degree of slow/fast decoupling. In fact, the basis vectors used to define the matrix might be found, in principle, by different means, if they can provide the ideal block-diagonalization of the eigenvalue matrix in a cost efficient way. The Computational Singular Perturbation [2] method offers a computational algorithm to achieve this goal. The CSP refinements converge to the right/left eigenvectors of $J(\boldsymbol{x}(t_n))$ if nonlinearities are neglected. In this case, we can rank the basis vectors according to the magnitude of the corresponding eigenvalues, to obtain

$$0 = \lambda_1 = \cdots = \lambda_E < |\lambda_{E+1}| \leq \cdots \leq |\lambda_{H-1}| \ll |\lambda_H| \leq \cdots \leq |\lambda_T| \ll |\lambda_{T+1}| \leq \cdots \leq |\lambda_{N+1}|, \tag{9}$$

where

$$\begin{aligned} 0 = \lambda_1 = \cdots = \lambda_E \quad & \text{identify the scales in } \mathbb{E}, \\ |\lambda_{E+1}| \leq \cdots \leq |\lambda_{H-1}| \quad & \text{identify the scales in } \mathbb{H}, \\ |\lambda_H| \leq \cdots \leq |\lambda_T| \quad & \text{identify the scales in } \mathbb{A}, \\ |\lambda_{T+1}| \leq \cdots \leq |\lambda_{N+1}| \quad & \text{identify the scales in } \mathbb{T}. \end{aligned} \tag{10}$$

As estimate of the time scale associated to an eigen-direction, we take the reciprocal of the magnitude of the corresponding eigenvalue.

The G-Scheme exploits the two archetypes for reduction introduced by Tikhonov[3] and Fenichel [4]: slow-invariant-manifold (SIM) and fast-fibers (FF), to define the adaptive reduction; the SIM and FF concepts are invoked to define the T(ail) and H(ead) subspaces, respectively; the concepts of SIM and FF are invoked on a local basis. The contributions of fast and slow scales are accounted for with SIM and FF algebraic corrections obtained through asymptotic analysis. Differently from other approaches, for the G-Scheme to be applicable it is not required that a global SIM exist, nor that the SIM dimension be constant or prescribed in advance. Similar comments apply for the exploitation of the FF.

Entropy Production and Time Scale Decomposition

Let us now assume that the dynamical system defined by Eq. (8) admits an entropy function (a state function), as defined in Eq. (6) that can be functionally expressed as a function of the state of the system, $\boldsymbol{x}$, as

$$s = s(\boldsymbol{x}). \tag{11}$$

The question addressed in this section is how the time rate of change of entropy, ds/dt, can be related to the fast, active, and and slow dynamics of Eq. (8).

[1] G stands for Grappa, an Italian liquor produced by distillation.

As customary, one can decompose

$$\boldsymbol{g} = \boldsymbol{g}_{\text{fast}} + \boldsymbol{g}_{\text{active}} + \boldsymbol{g}_{\text{slow}} = \boldsymbol{a}_r\, \boldsymbol{f}^r + \boldsymbol{a}_a\, \boldsymbol{f}^a + \boldsymbol{a}_s\, \boldsymbol{f}^s \tag{12}$$

where the mode amplitudes associated with the three subspaces are defined as

$$\boldsymbol{f}^r := \boldsymbol{b}^r \cdot \boldsymbol{g} \quad \boldsymbol{f}^a := \boldsymbol{b}^a \cdot \boldsymbol{g} \quad \boldsymbol{f}^s := \boldsymbol{b}^s \cdot \boldsymbol{g} \tag{13}$$

Now applying the chain rule to write the time rate of change of entropy as

$$\boxed{\frac{\mathrm{ds}}{\mathrm{dt}} = \boldsymbol{\nabla} s \cdot \frac{\mathrm{d}\boldsymbol{x}}{\mathrm{dt}} = \boldsymbol{\nabla} s \cdot \boldsymbol{g}(\boldsymbol{x}) = (\boldsymbol{\nabla} s \cdot \boldsymbol{a}_r)\, \boldsymbol{f}^r + (\boldsymbol{\nabla} s \cdot \boldsymbol{a}_a)\, \boldsymbol{f}^a + (\boldsymbol{\nabla} s \cdot \boldsymbol{a}_s)\, \boldsymbol{f}^s} \tag{14}$$

Remark #1
Eq. (14) suggests that entropy production is controlled by the magnitudes of the mode amplitudes spanning the fast, active, and slow subspaces, with weights that depend on the projection of the entropy gradient onto each of these subspaces.

The Slow Invariant Manifold (SIM) of Eq. (8) is defined as the locus of state points $\boldsymbol{x}$ which satisfy the algebraic condition:

$$\boldsymbol{f}^r(\boldsymbol{x}) \approx \boldsymbol{0} \tag{15}$$

In addition, as shown later, the contribution of the slow subspace to the the time rate of change of entropy is usually small, that is

$$|\boldsymbol{f}^s| \ll 1 \tag{16}$$

This means that the contribution of the fast and/or slow scales to the time rate of change of entropy is negligible while moving along the SIM, independently of the details of the state function defined in Eq. (11).

Subsequently, the implication is that the time rate of change of entropy is mostly contributed from the active scales

$$\boxed{\frac{\mathrm{ds}}{\mathrm{dt}} \approx (\boldsymbol{\nabla} s \cdot \boldsymbol{a}_a)\, \boldsymbol{f}^a} \tag{17}$$

From Eq. (17), the process is isentropic if

$$\boldsymbol{\nabla} s \cdot \boldsymbol{a}_a \approx 0 \tag{18}$$

that is, when $\boldsymbol{\nabla} s$ is orthogonal to $\boldsymbol{a}_a$.

Note that the time rate of change of entropy can be zero away from the SIM or when $|\boldsymbol{f}^s| \approx O(1)$, if it holds $\boldsymbol{\nabla} s \cdot \boldsymbol{a}_r \neq 0$ and $\boldsymbol{\nabla} s \cdot \boldsymbol{a}_s \neq 0$, that is, when $\boldsymbol{\nabla} s$ is not orthogonal to $\boldsymbol{a}_r$ and $\boldsymbol{a}_s$.

These results apply to any state function given that we have not used any other entropy - specific property to reach this conclusion.

Entropy Production and the G-Scheme
In this section, we aim at finding a direct link between time scales and entropy production. According with the G-Scheme framework, we will proceed by first performing a change of variables in Eq. (8) from time t to τ and from $\boldsymbol{x}$ to $\delta\boldsymbol{x}$ defined by

$$t = t_n + \tau \qquad \boldsymbol{x} = \boldsymbol{x}_n + \delta\boldsymbol{x} \tag{19}$$

where $\boldsymbol{x}_n = \varphi_{t_n}(\boldsymbol{x}_0)$. Next, we will account for the contribution of the slow, active, and fast subspaces to the time rate of change of $\delta\boldsymbol{x}$, according with the estimates provided by the G-Scheme framework.

Let us start by first projecting $\delta\boldsymbol{x}$ over the three subspaces to obtain the following expansion

$$\begin{aligned}\delta\boldsymbol{x} &= (\boldsymbol{a}_r\boldsymbol{b}^r + \boldsymbol{a}_a\boldsymbol{b}^a + \boldsymbol{a}_s\boldsymbol{b}^s)\cdot\delta\boldsymbol{x} = \\ &\boldsymbol{a}_r\left(\boldsymbol{b}^r\cdot\delta\boldsymbol{x}\right) + \boldsymbol{a}_a\left(\boldsymbol{b}^a\cdot\delta\boldsymbol{x}\right) + \boldsymbol{a}_s\left(\boldsymbol{b}^s\cdot\delta\boldsymbol{x}\right) = \\ &\boldsymbol{a}_r\delta\boldsymbol{\xi}^r + \boldsymbol{a}_a\delta\boldsymbol{\xi}^a + \boldsymbol{a}_s\delta\boldsymbol{\xi}^s.\end{aligned} \tag{20}$$

where a new set of curvilinear coordinates $\delta\boldsymbol{\xi}^j$ is introduced to describe the changes of the vector $\delta\boldsymbol{x}$ within the three subspaces spanned by $\boldsymbol{a}_r$, $\boldsymbol{a}_a$, $\boldsymbol{a}_s$, according with the definitions $\delta\boldsymbol{\xi}^r := \boldsymbol{b}^r\cdot\delta\boldsymbol{x}, \delta\boldsymbol{\xi}^a := \boldsymbol{b}^a\cdot\delta\boldsymbol{x}, \delta\boldsymbol{\xi}^s := \boldsymbol{b}^s\cdot\delta\boldsymbol{x}$.

The dynamics of $\delta\boldsymbol{x}$ starting from the point $\boldsymbol{x}_n$ and within a time period $\delta\tau$ having an order of magnitude

$$\delta\tau \approx O\left(\frac{1}{|\boldsymbol{\lambda}_a|}\right) \tag{21}$$

is described by

$$\begin{aligned}\frac{d\left(\boldsymbol{x}_n+\delta\boldsymbol{x}\right)}{\mathrm{d}\tau} &= \boldsymbol{g}\left(\boldsymbol{x}_n+\delta\boldsymbol{x}\right) \qquad \delta\boldsymbol{x}(\tau=0)=\boldsymbol{0} \\ \frac{d(\delta\boldsymbol{x})}{\mathrm{d}\tau} &\approx \boldsymbol{g}\left(\boldsymbol{x}_n\right) + \boldsymbol{\nabla}\boldsymbol{g}\left(\boldsymbol{x}_n\right)\cdot\delta\boldsymbol{x} = \boldsymbol{g}\left(\boldsymbol{x}_n\right) + J_{\boldsymbol{x}_n}\cdot\delta\boldsymbol{x} \qquad \delta\boldsymbol{x}(\tau=0)=\boldsymbol{0}\end{aligned} \tag{22}$$

where we used the definition

$$J_{\boldsymbol{x}_n} := \boldsymbol{\nabla}\boldsymbol{g}\left(\boldsymbol{x}_n\right) \tag{23}$$

Invoking the G-Scheme decomposition of the Jacobian matrix

$$J_{\boldsymbol{x}_n} = A_{\boldsymbol{x}_n}\Lambda_{\boldsymbol{x}_n}B_{\boldsymbol{x}_n} = \boldsymbol{a}_r\boldsymbol{\lambda}_r\boldsymbol{b}^r + \boldsymbol{a}_a\boldsymbol{\lambda}_a\boldsymbol{b}^a + \boldsymbol{a}_s\boldsymbol{\lambda}_s\boldsymbol{b}^s \tag{24}$$

allow us to write

$$\frac{d(\delta\boldsymbol{x})}{\mathrm{d}\tau} \approx \boldsymbol{g}\left(\boldsymbol{x}_n\right) + \left(A_{\boldsymbol{x}_n}\Lambda_{\boldsymbol{x}_n}B_{\boldsymbol{x}_n}\right)\cdot\delta\boldsymbol{x} \approx \boldsymbol{g}\left(\boldsymbol{x}_n\right) + \left(\boldsymbol{a}_r\boldsymbol{\lambda}_r\boldsymbol{b}^r + \boldsymbol{a}_a\boldsymbol{\lambda}_a\boldsymbol{b}^a + \boldsymbol{a}_s\boldsymbol{\lambda}_s\boldsymbol{b}^s\right)\cdot\delta\boldsymbol{x} \tag{25}$$

To leading order, one can express the entropy $s(\boldsymbol{x})$ at $\boldsymbol{x} = \boldsymbol{x}_n + \delta\boldsymbol{x}$ as

$$s(\boldsymbol{x}) = s(\boldsymbol{x}_n+\delta\boldsymbol{x}) \approx s(\boldsymbol{x}_n) + \boldsymbol{\nabla}s\,\delta\boldsymbol{x} \tag{26}$$

Therefore, the time rate of change of entropy can be written as

$$\frac{ds(\boldsymbol{x})}{d\tau} \approx \frac{d}{d\tau}(s(\boldsymbol{x}_n)) + \boldsymbol{\nabla}s\,\frac{d(\delta\boldsymbol{x})}{d\tau} = \boldsymbol{\nabla}s\,\frac{d(\delta\boldsymbol{x})}{d\tau} \tag{27}$$

In the formula above, we can replace the time derivative of $\delta\boldsymbol{x}$ using Eq. (22) to obtain

$$\begin{aligned}\frac{ds}{d\tau} &= \boldsymbol{\nabla}s\cdot\frac{d(\delta\boldsymbol{x})}{d\tau} = \boldsymbol{\nabla}s\cdot\left(\boldsymbol{g}\left(\boldsymbol{x}_n\right) + A_{\boldsymbol{x}_0}\Lambda_{\boldsymbol{x}_0}B_{\boldsymbol{x}_0}\cdot\delta\boldsymbol{x}\right) = \\ &\boldsymbol{\nabla}s\cdot\boldsymbol{g}\left(\boldsymbol{x}_n\right) + \boldsymbol{\nabla}s\cdot A_{\boldsymbol{x}_n}\Lambda_{\boldsymbol{x}_n}B_{\boldsymbol{x}_n}\cdot\delta\boldsymbol{x}.\end{aligned} \tag{28}$$

We can further elaborate Eqs. (25) and (28) to obtain

$$\begin{aligned}
&(\boldsymbol{\nabla} s \cdot A_{\boldsymbol{x}_n})\, \Lambda_{\boldsymbol{x}_n}\, (B_{\boldsymbol{x}_n} \cdot \delta \boldsymbol{x}) = \\
&(\boldsymbol{\nabla} s \cdot \boldsymbol{a}_r)\, \boldsymbol{\lambda}_r\, (\boldsymbol{b}^r \cdot \delta \boldsymbol{x}) + (\boldsymbol{\nabla} s \cdot \boldsymbol{a}_a)\, \boldsymbol{\lambda}_a\, (\boldsymbol{b}^a \cdot \delta \boldsymbol{x}) + (\boldsymbol{\nabla} s \cdot \boldsymbol{a}_s)\, \boldsymbol{\lambda}_s\, (\boldsymbol{b}^s \cdot \delta \boldsymbol{x}) = \\
&(\boldsymbol{\nabla} s \cdot \boldsymbol{a}_r)\, \boldsymbol{\lambda}_r \delta \boldsymbol{\xi}^r + (\boldsymbol{\nabla} s \cdot \boldsymbol{a}_a)\, \boldsymbol{\lambda}_a \delta \boldsymbol{\xi}^a + (\boldsymbol{\nabla} s \cdot \boldsymbol{a}_s)\, \boldsymbol{\lambda}_s \delta \boldsymbol{\xi}^s.
\end{aligned} \tag{29}$$

Let now consider the contribution of the 3 subspaces to the time rate of change of entropy

$$\begin{aligned}
&(\boldsymbol{\nabla} s \cdot \boldsymbol{a}_r)\, \boldsymbol{\lambda}_r \delta \boldsymbol{\xi}^r \\
&(\boldsymbol{\nabla} s \cdot \boldsymbol{a}_a)\, \boldsymbol{\lambda}_a \delta \boldsymbol{\xi}^a \\
&(\boldsymbol{\nabla} s \cdot \boldsymbol{a}_s)\, \boldsymbol{\lambda}_s \delta \boldsymbol{\xi}^s
\end{aligned} \tag{30}$$

According with the G-Scheme framework, we can estimate the magnitude of the change of the slow curvilinear coordinate, $\delta \boldsymbol{\xi}^s$, as

$$\delta \boldsymbol{\xi}^s \approx \delta \tau\; \boldsymbol{b}^s \cdot \boldsymbol{g}\,(\boldsymbol{x}_n) = \delta \tau\; \boldsymbol{f}^s\,(\boldsymbol{x}_n)\,, \tag{31}$$

of the change of the active curvilinear coordinate, $\delta \boldsymbol{\xi}^a$, as

$$\delta \boldsymbol{\xi}^a \approx \boldsymbol{b}^a \cdot \boldsymbol{g}\,(\boldsymbol{x}_n + \boldsymbol{a}_a \delta \boldsymbol{\xi}^a)\, \delta \tau \approx \boldsymbol{b}^a \cdot \boldsymbol{g}\,(\boldsymbol{x}_n)\, \delta \tau + \boldsymbol{b}^a \cdot J_{\boldsymbol{x}_n} \boldsymbol{a}_a \delta \boldsymbol{\xi}^a \delta \tau \approx (\boldsymbol{f}^a\,(\boldsymbol{x}_n) + \boldsymbol{\lambda}_a \delta \boldsymbol{\xi}^a)\, \delta \tau \tag{32}$$

which yields an implicit definition of $\delta \boldsymbol{\xi}^a$

$$\begin{aligned}
&(I - \boldsymbol{\lambda}_a \delta \tau) \delta \boldsymbol{\xi}^a = \boldsymbol{f}^a\,(\boldsymbol{x}_n)\, \delta \tau \\
&\delta \boldsymbol{\xi}^a = (I - \boldsymbol{\lambda}_a \delta \tau)^{-1}\, \boldsymbol{f}^a\,(\boldsymbol{x}_n)\, \Delta \mathrm{t},
\end{aligned} \tag{33}$$

and of the change of the fast curvilinear coordinate, $\delta \boldsymbol{\xi}^r$, when $\boldsymbol{x}_0$ is on the SIM as

$$\delta \boldsymbol{\xi}^r_{SIM}\,(\boldsymbol{x}) \approx -\left(\boldsymbol{b}^r J_{\boldsymbol{x}_n} \boldsymbol{a}_r\right)^{-1} \boldsymbol{b}^r \cdot \boldsymbol{g}\,(\boldsymbol{x}) \approx -\boldsymbol{\lambda}_r^{-1} \boldsymbol{f}^r\,(\boldsymbol{x}) \approx 0 \tag{34}$$

where

$$\boldsymbol{\lambda}_r = \boldsymbol{b}^r\, J_{\boldsymbol{x}_n} \boldsymbol{a}_r \tag{35}$$

and the amplitude of the fast modes, $\boldsymbol{f}^r(\boldsymbol{x})$, is negligible when $\boldsymbol{x}$ is taken on the SIM

$$\boldsymbol{f}^r\,(\boldsymbol{x}) = \boldsymbol{b}^r \cdot \boldsymbol{g}\,(\boldsymbol{x}) \approx 0 \tag{36}$$

so that on the SIM

$$\delta \boldsymbol{\xi}^r_{SIM} \approx 0 \tag{37}$$

The second term in (25) can thus be estimated as:

$$\begin{aligned}
&(\boldsymbol{\nabla} s \cdot R_{\boldsymbol{x}_n})\, \Lambda_{\boldsymbol{x}_n}\, (B_{\boldsymbol{x}_n} \cdot \delta \boldsymbol{x}) = \\
&(\boldsymbol{\nabla} s \cdot \boldsymbol{a}_r)\; \boldsymbol{\lambda}_r \delta \boldsymbol{\xi}^r_{SIM} + (\boldsymbol{\nabla} s \cdot \boldsymbol{a}_a)\; \boldsymbol{\lambda}_a \delta \boldsymbol{\xi}^a + (\boldsymbol{\nabla} s \cdot \boldsymbol{a}_s)\; \boldsymbol{\lambda}_s \delta \boldsymbol{\xi}^s = \\
&-(\boldsymbol{\nabla} s \cdot \boldsymbol{a}_r) \cdot\; \boldsymbol{f}^r\,(\boldsymbol{x}_n) + (\boldsymbol{\nabla} s \cdot \boldsymbol{a}_a) \cdot \boldsymbol{\lambda}_a\, (I - \boldsymbol{\lambda}_a \delta \tau)^{-1}\, \boldsymbol{f}^a\,(\boldsymbol{x}_n)\, \Delta \mathrm{t} + (\boldsymbol{\nabla} s \cdot \boldsymbol{a}_s) \cdot \boldsymbol{\lambda}_s \delta \tau\, \boldsymbol{f}^s\,(\boldsymbol{x}_n) = \\
&-(\boldsymbol{\nabla} s \cdot \boldsymbol{a}_r) \cdot\; \boldsymbol{f}^r\,(\boldsymbol{x}_n) + (\boldsymbol{\nabla} s \cdot \boldsymbol{a}_a) \cdot \frac{\boldsymbol{\lambda}_a}{|\boldsymbol{\lambda}_a|}\, (I - \boldsymbol{\lambda}_a \delta \tau)^{-1}\, \boldsymbol{f}^a\,(\boldsymbol{x}_n) + (\boldsymbol{\nabla} s \cdot \boldsymbol{a}_s) \cdot \frac{\boldsymbol{\lambda}_s}{|\boldsymbol{\lambda}_a|}\, \boldsymbol{f}^s\,(\boldsymbol{x}_n)
\end{aligned} \tag{38}$$

After these considerations, the time rate of change of entropy can be rewritten as

$$\begin{aligned}\frac{ds}{d\tau} &= \boldsymbol{\nabla} s \cdot \frac{d(\delta \boldsymbol{x})}{d\tau} = \boldsymbol{\nabla} s \cdot \boldsymbol{g}\left(\boldsymbol{x}_n\right) + \\ &+ \left(\boldsymbol{\nabla} s \cdot \boldsymbol{a}_s\right) \cdot \frac{\boldsymbol{\lambda}_s}{|\boldsymbol{\lambda}_a|}\, \boldsymbol{f}^s\left(\boldsymbol{x}_n\right) \\ &+ \left(\boldsymbol{\nabla} s \cdot \boldsymbol{a}_a\right) \cdot \frac{\boldsymbol{\lambda}_a}{|\boldsymbol{\lambda}_a|}\, \left(I - \boldsymbol{\lambda}_a \delta\tau\right)^{-1} \boldsymbol{f}^a\left(\boldsymbol{x}_n\right) + \\ &- \left(\boldsymbol{\nabla} s \cdot \boldsymbol{a}_r\right) \cdot\, \boldsymbol{f}^r\left(\boldsymbol{x}_n\right)\end{aligned} \tag{39}$$

We can also elaborate on the first term by projecting $\boldsymbol{g}\left(\boldsymbol{x}_n\right)$ in the 3 subspaces (as in Eq.(12))

$$\boldsymbol{\nabla} s \cdot \boldsymbol{g}\left(\boldsymbol{x}_n\right) = \boldsymbol{\nabla} s \cdot \left(\boldsymbol{a}_r\, \boldsymbol{f}^r\left(\boldsymbol{x}_n\right) + \boldsymbol{a}_a\, \boldsymbol{f}^a\left(\boldsymbol{x}_n\right) + \boldsymbol{a}_s\, \boldsymbol{f}^s\left(\boldsymbol{x}_n\right)\right) \tag{40}$$

Therefore, Eq.(39) becomes:

$$\boxed{\begin{aligned}\frac{ds}{d\tau} &= \boldsymbol{\nabla} s \cdot \left(\boldsymbol{a}_r\, \boldsymbol{f}^r\left(\boldsymbol{x}_n\right) + \boldsymbol{a}_a\, \boldsymbol{f}^a\left(\boldsymbol{x}_n\right) + \boldsymbol{a}_s\, \boldsymbol{f}^s\left(\boldsymbol{x}_n\right)\right) + \\ &+ \left(\boldsymbol{\nabla} s \cdot \boldsymbol{a}_s\right) \cdot \frac{\boldsymbol{\lambda}_s}{|\boldsymbol{\lambda}_a|}\, \boldsymbol{f}^s\left(\boldsymbol{x}_n\right) \\ &+ \left(\boldsymbol{\nabla} s \cdot \boldsymbol{a}_a\right) \cdot \frac{\boldsymbol{\lambda}_a}{|\boldsymbol{\lambda}_a|}\, \left(I - \boldsymbol{\lambda}_a \delta\tau\right)^{-1} \boldsymbol{f}^a\left(\boldsymbol{x}_n\right) + \\ &- \left(\boldsymbol{\nabla} s \cdot \boldsymbol{a}_r\right) \cdot\, \boldsymbol{f}^r\left(\boldsymbol{x}_n\right)\end{aligned}} \tag{41}$$

which can be recast as:

$$\begin{aligned}\frac{ds}{d\tau} &= \left(\boldsymbol{\nabla} s \cdot \boldsymbol{a}_s\right) \cdot \left(I + \frac{\boldsymbol{\lambda}_s}{|\boldsymbol{\lambda}_a|}\right) \boldsymbol{f}^s\left(\boldsymbol{x}_n\right) \\ &+ \left(\boldsymbol{\nabla} s \cdot \boldsymbol{a}_a\right) \cdot \left(I + \frac{\boldsymbol{\lambda}_a}{|\boldsymbol{\lambda}_a|}\, \left(I - \boldsymbol{\lambda}_a \delta\tau\right)^{-1}\right) \boldsymbol{f}^a\left(\boldsymbol{x}_n\right) + \\ &+ \left(\boldsymbol{\nabla} s \cdot \boldsymbol{a}_r\right) \cdot \left(\boldsymbol{f}^r\left(\boldsymbol{x}_n\right) - \, \boldsymbol{f}^r\left(\boldsymbol{x}_n\right)\right)\end{aligned} \tag{42}$$

Remark #2
Eqs. (41) and (42) are the sought after result that relates entropy production to the time scales associated with the slow, active, and fast subspaces.

Let us now assume that there exists a large spectral gap between the slow and active subspaces so that $|\boldsymbol{\lambda}_s| \ll |\boldsymbol{\lambda}_a|$, $\boldsymbol{\lambda}_a/|\boldsymbol{\lambda}_a| \approx O(1)$. Under these assumptions, Eq. (42) simplifies into:

$$\boxed{\frac{ds}{d\tau} \approx \left(\boldsymbol{\nabla} s \cdot \boldsymbol{a}_s\right) \cdot \boldsymbol{f}^s\left(\boldsymbol{x}_n\right) + \left(\boldsymbol{\nabla} s \cdot \boldsymbol{a}_a\right) \cdot \left(I + \, \left(I - \boldsymbol{\lambda}_a \delta\tau\right)^{-1}\right) \boldsymbol{f}^a\left(\boldsymbol{x}_n\right)} \tag{43}$$

In summary, inspection of Eq. (43) reveals that the time rate of change of entropy is zero if the following two conditions hold

$$\begin{aligned}&\boldsymbol{\nabla} s \text{ is orthogonal to } \boldsymbol{a}_s \text{ or } \boldsymbol{f}^s\left(\boldsymbol{x}_n\right) = 0 \\ &\boldsymbol{\nabla} s \text{ is orthogonal to } \boldsymbol{a}_a \text{ or } \boldsymbol{f}^a\left(\boldsymbol{x}_n\right) = 0\end{aligned} \tag{44}$$

The fast subspace does not contribute to the time rate of change of entropy when the state is on the SIM.

The contribution of the slow subspace to the time rate of change of entropy

$$(\boldsymbol{\nabla} s \cdot \boldsymbol{a}_s) \cdot \left(I + \frac{\boldsymbol{\lambda}_s}{|\boldsymbol{\lambda}_a|} \right) \boldsymbol{f}^s (\boldsymbol{x}_n)$$

is proportional to the ratio $|\boldsymbol{\lambda}_s|/|\boldsymbol{\lambda}_a|$ and to the magnitude of the slow mode amplitude $\boldsymbol{f}^s (\boldsymbol{x}_n)$.

Results

The specific test case considered refers to a methane/air system, using GRI 3.0 kinetics (53 species). The batch reactor model is adiabatic and at constant volume. The initial conditions for the test case are defined by prescribing the initial temperature $T_0 = 1000$ K and pressure $p_0 = 1$ atm of a stoichiometric mixture of reactants. The constant density in Eq. (1) is set on the basis of the thermal equation of state.

Figure 1 shows the evolution of temperature (solid, black line) as a function of the number of iteration steps (to avoid the compression of the plot about the reaction time). On the same figure, we plot the evolution of the dimension A of the active subspace (green solid line) obtained by subtracting H (blue line) from T (red line), where H and T are the mode numbers corresponding to $|\lambda_H|$ and $|\lambda_T|$, respectively. The dimension of the active subspace also corresponds to the number of non-stiff ODEs solved by the G-Scheme. The modes comprised between 5 and H-1 span the slow subspace, those between H and T the active subspace, and those between T+1 and N+1 the fast subspace.

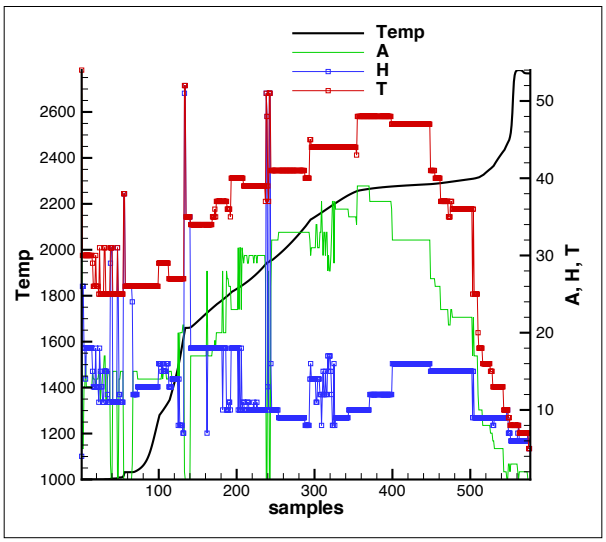

Figure 1: Time evolution of the dimension of the active (green), slow (blue), and fast (red) subspaces; temperature (solid black line); $rtol = 10^{-3}$.

Figure 2 shows the time evolution of the reciprocal of the modulus of the (complex) eigenvalues of the 55 modes as a function of the number of iteration steps. On the same figure, we plot the evolution of the characteristic scales of the G-Scheme, namely, the reciprocal of $|\lambda_{H-1}|$ (green), $|\lambda_H|$ (red), $|\lambda_T|$ (cyan), $|\lambda_{T+1}|$ (blue), and $|\lambda_{N+1}|$ (black). The blue solid line reports the entropy evolution. The slow/active scale gap is is visually comprised between the green and red lines, while the active/fast gap is between the cyan and blue lines. The black line marks the fastest time scale at all times. The spectral width of the fast subspace is between the black and blue lines. The width of the active

subspace is between the cyan and red lines. The width of the slow subspace is above the red line. The invariant subspace is associated with the randomly scattered markers visible at very large time scales.

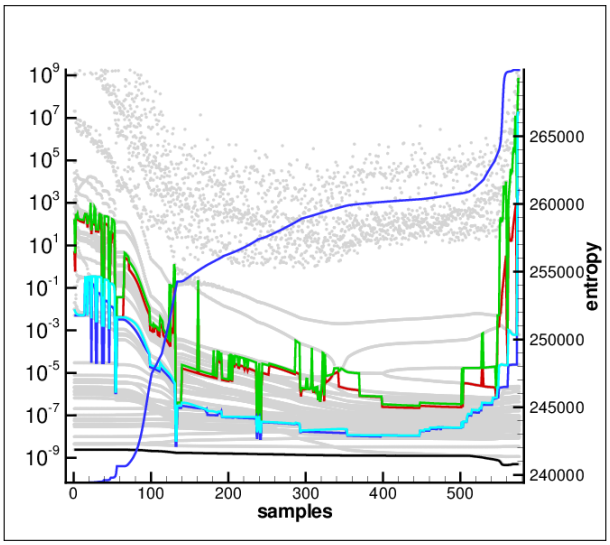

Figure 2: Reciprocal of the modulus of the (complex) eigenvalues (light grey markers); reciprocal of $|\lambda_{H-1}|$ (green), $|\lambda_H|$ (red), $|\lambda_T|$ (cyan), $|\lambda_{T+1}|$ (blue), and $|\lambda_{N+1}|$ (black); the red solid line reports the entropy evolution; $rtol = 10^{-3}$.

The quantitative assessment of the relative contribution to the rate of entropy production from the slow, active, and fast subspaces is carried out by considering that the entropy of the mixture is a state function of temperature and composition. Therefore, during the numerical integration of the batch reactor model, we evaluated the entropy of the mixture before and after each of the changes of the system state due to the slow (Δs_h), active (Δs_a), and fast (Δs_t) subspaces. With these definitions, we introduced the following definitions:

$$\begin{aligned} s_\alpha(t_n) &= s_\alpha(t_{n-1}) + \Delta s_\alpha(t_n) \qquad \alpha = h, a, t \\ s(t_n) &= s_h(t_n) + s_a(t_n) + s_t(t_n) \end{aligned} \tag{45}$$

where $s_\alpha(t_0) = s(T_0, p_0, Y_{j,0})$.

Figure 3 shows the time evolution of the contribution to the entropy of the mixture from the slow, active, and fast subspaces as obtained using three different accuracy levels ($rtol = 10^{-3}, 10^{-4}, 10^{-5}$), while Fig. 4 shows the entropy contribution of each subspace scaled with respect to the overall contribution ($s_\alpha(t_n)/s(t_n)$, with $\alpha = a, h, t$).

It is apparent that the active subspace contribution is always very close to 100%, while the slow contribution is generally larger than the fast contribution.

The sensitivity to the accuracy level of the contribution to the entropy of the mixture can be appreciated with the help of Fig. 5, which indicates that the magnitude of the overall entropy contribution, that is, evaluated at large times, of the fast subspace is of the same order of the accuracy level specified by the user. Instead the overall entropy contribution of the slow subspace is always smaller than the active contribution, but it does not seem to depend much on the accuracy level specified by the user.

Figure 6 shows that the relative contribution to the rate of entropy production ($\Delta s_\alpha(t_n)$ / $\Delta s(t_n)$) of the slow and fast subspaces are approximately 10^{-3} and 10^{-4}, respectively, whereas that of the active subspace is always of order one. This indicates that the con-

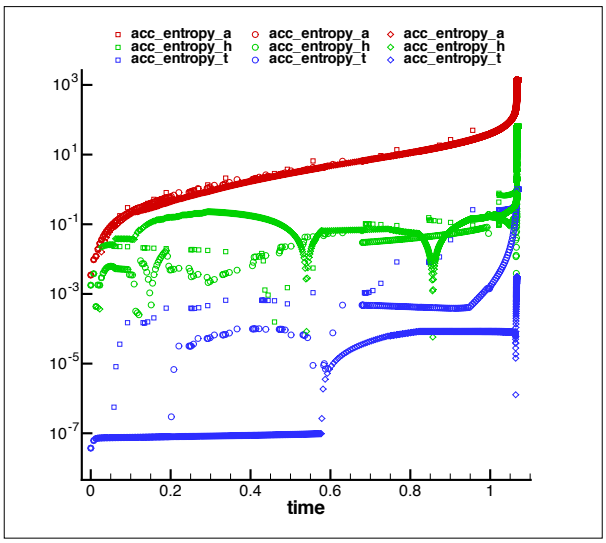

Figure 3: Contribution to the entropy of the mixture from the slow ($s_h(t_n)$, green), active ($s_a(t_n)$, red), and fast ($s_t(t_n)$, blue) subspaces, as obtained using three different accuracy levels ($rtol = 10^{-3}$ (square markers), 10^{-4} (circles), 10^{-5} (diamonds)).

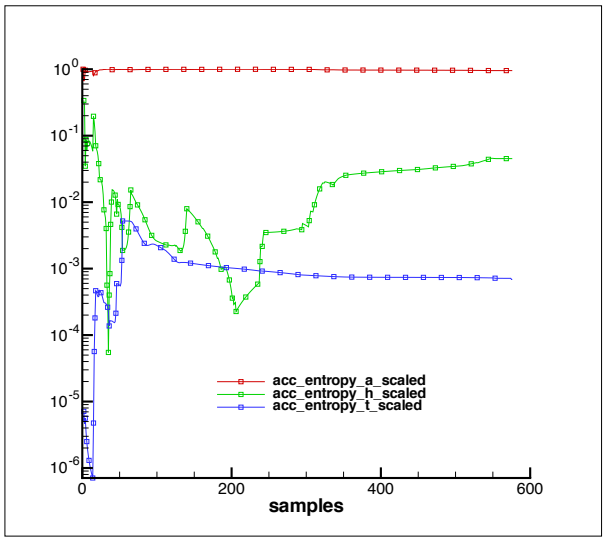

Figure 4: Contribution to the entropy of the mixture from the slow ($s_h(t_n)/s(t_n)$, green), active ($s_a(t_n)/s(t_n)$, red), and fast ($s_t(t_n)/s(t_n)$, blue) subspaces scaled with respect to the overall contribution ($rtol = 10^{-3}$).

tribution to the rate of entropy production of the fast subspace is always negligible with respect to that of the active subspace, whereas that of the slow subspace can occasionally becomes comparable to that of the active subspace within the reaction period of the auto-ignition process.

Acknowledgment

MV acknowledges the support of the Italian Ministry of University and Research (MIUR).

*

References

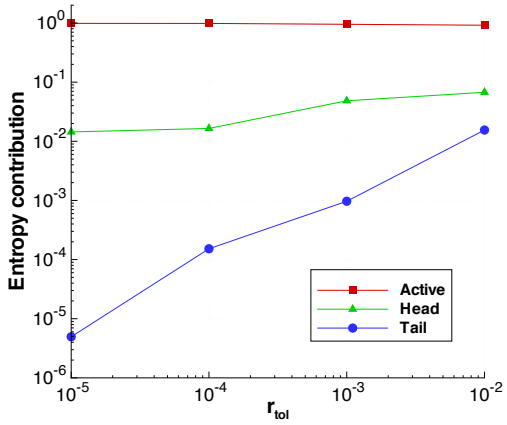

Figure 5: Overall entropy production per each subspace; slow ($s_h(t_\infty)$, green), active ($s_a(t_\infty)$, red), and fast ($s_t(t_\infty)$, blue) subspaces.

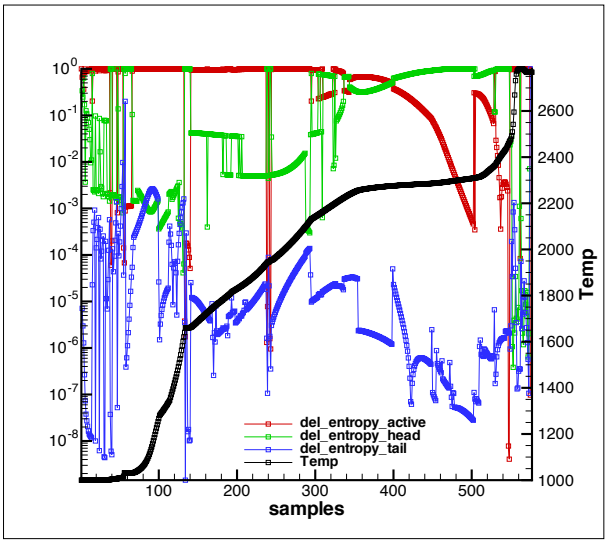

Figure 6: Contribution to the rate of change of entropy of the mixture from the slow ($\Delta s_h(t_n)/\Delta s(t_n)$, green), active ($\Delta s_a(t_n)/\Delta s(t_n)$, red), and fast ($\Delta s_t(t_n)/\Delta s(t_n)$, blue) subspaces ($rtol = 10^{-3}$).

[1] Valorani, M., Paolucci, S., "The G-Scheme: A framework for multi-scale adaptive model reduction", *Journal of Computational Physics* 228:4665–4701 (2009).

[2] Lam, S.H., Goussis, D.A., "The CSP method for simplifying kinetics", *International Journal of Chemical Kinetics* 26:461–486 (1994).

[3] Tikhonov, A., "Systems of differential equations containing a small parameter multiplying the derivative", *Mat. Sb.* 31:575–586 (1952).

[4] Fenichel, N., "Geometric singular perturbation theory for ordinary differential equations", *J. Diff. Eqs.* 31:53–98 (1979).